Synthesis and structures of platinum diphenylacetylene and dithiolate complexes bearing diphosphinidenecyclobutene ligands (DPCB-Y)†‡§

Yumiko Nakajima, Mitsuharu Nakatani, Kyohei Hayashi, Yu Shiraishi, Ryo Takita, Masaaki Okazaki and Fumiyuki Ozawa*

Received (in Victoria, Australia) 13th February 2010, Accepted 27th April 2010
DOI: 10.1039/c0nj00118j

A series of platinum complexes of the type [Pt(D)(A)] having two kinds of π-conjugated ligand systems with donor and acceptor properties are prepared, using *p*-substituted diphenylacetylenes (tolan-X; X = OMe, H, CF_3), 1,2-benzenedithiolato (bdt) and 1,3-dithia-2-thione-4,5-dithiolato (dmit) as π-donor ligands (D), and 1,2-diaryl-3,4-bis[(2,4,6-tri-*tert*-butylphenyl)phosphinidene]-cyclobutenes (DPCB-Y; diaryl = $2C_6H_4$-*p*-Y (Y = OMe, H, CF_3), biphenyl-2,2′-diyl) as π-acceptor ligands (A). The electronic structures of the resulting complexes are examined in detail to investigate π-orbital interaction occurring in DPCB-Y complexes with a low-coordinate phosphorus ligand. The ^{31}P NMR chemical shifts are highly sensitive to the Pt–P distances of the complexes, and linearly correlated with the bond lengths. The UV-vis absorption spectra of [Pt(tolan-X)(DPCB-Y)] display π–π* transitions in the visible region, which are shifted to longer wavelengths as the electron-donating ability of X and electron-withdrawing ability of Y increase, respectively. The complex [Pt(tolan-OMe)(DPCB-CF_3)] with a donor–acceptor combination of substituents exhibits particularly low-energy absorption. The absorption is further red-shifted for [Pt(bdt)(DPCB-phen)] and [Pt(dmit)(DPCB-phen)] having dithiolates as strong π-donor ligands.

Introduction

Low-coordinate phosphorus compounds have attracted recent interest in organometallic chemistry owing to their unique ligand properties differing significantly from common tertiary phosphines.[1] We have reported that 1,2-diaryl-3,4-bis-[(2,4,6-tri-*tert*-butylphenyl)phosphinidene]cyclobutenes (DPCB-Y, Fig. 1) having an extended π-conjugated system with two P=C bonds serve as particularly useful ligands, leading to highly efficient catalyses in combination with group 8, 9 and 10 metals.[2] Representative examples include hydroamination of 1,3-dienes (Pd),[3] dehydrative allylation with allylic alcohols (Pd),[4] conjugate addition of benzyl carbamate to α,β-unsaturated ketones (Pd, Rh)[5] and *Z*-selective hydrosilylation of alkynes (Ru).[6] In this connection, we have been interested in evaluating electronic properties of DPCB-Y ligands in real coordination systems.

DPCB-Y undergoes bidentate coordination *via* two types of orbital interaction with transition metals. One is σ-donation of lone-pair electrons on the phosphorus to vacant metal orbitals, and the other is π-back donation from occupied metal d orbitals to the π* orbitals of DPCB-Y. The previous study of [$PtMe_2$(DPCB-Y)] revealed intermediate σ-donating ability between diphosphanes and diimines.[7] On the other hand, although the structural variation between uncoordinated and coordinated ligands was consistent with the occurrence of π-back donation from platinum, the π-accepting abilities of DPCB-Y ligands remained to be explored.

More recently, we examined the electronic structures of [Pt(alkyne)(DPCB-phen)] complexes by UV-vis absorption spectroscopy and found the occurrence of extended π-conjugation among the platinum, alkyne and DPCB-phen ligand.[8] It was suggested that the π-conjugation involves dπ–pπ interaction between platinum and the out-of-plane π* of alkyne ligand ($\pi_\perp$: the alkyne π* orbital perpendicular to the coordination plane), while such orbital interaction has been known to be insignificant in most cases, because the platinum dπ orbital is occupied and undergoes repulsive interaction with the alkyne $\pi_\perp$ orbital.[9] We reasoned that donor–acceptor interaction[10] between the electron-rich pπ

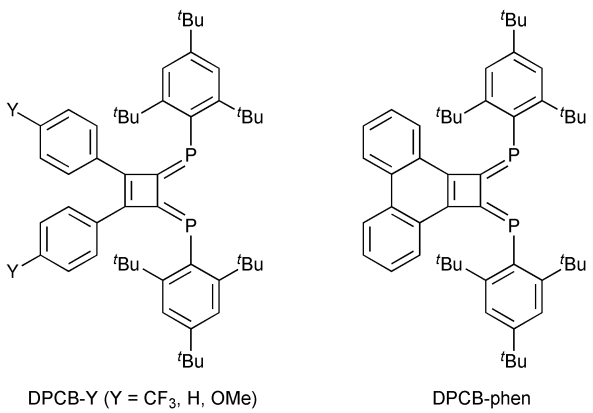

Fig. 1 Structures of DPCB-Y ligands.

International Research Center for Elements Science (IRCELS), Institute for Chemical Research, Kyoto University, Uji, Kyoto 611-0011, Japan. E-mail: ozawa@scl.kyoto-u.ac.jp
† This paper is dedicated to the memory of the late Professor Pascal Le Floch, Ecole Polytechnique.
‡ This article is part of a themed issue on Main Group chemistry.
§ Electronic supplementary information (ESI) available: Details of DFT calculations. CCDC reference numbers 735887 and 765285–765289. For ESI and crystallographic data in CIF or other electronic format see DOI: 10.1039/c0nj00118j

Table 1 List of the complexes employed in this study

X	Y	
OMe	OMe	**1a**
H	OMe	**1b**
CF_3	OMe	**1c**
OMe	H	**2a**
H	H	**2b**
CF_3	H	**2c**
OMe	CF_3	**3a**
H	CF_3	**3b**
CF_3	CF_3	**3c**
OMe	phen	**4a**
H	phen	**4b**
[Pt(bdt)(DPCB-H)]		**5a**
[Pt(dmit)(DPCB-H)]		**5b**
[Pt(bdt)(DPCB-phen)]		**6a**
[Pt(dmit)(DPCB-phen)]		**6b**

bdt = 1,2-benzenedithiolato, dmit = 1,3-dithia-2-thione-4,5-dithiolato.

system of alkyne and the electron-poor pπ system of DPCB-phen facilitates the π-conjugation through the dπ orbital of platinum.

To investigate further the π-orbital interaction in DPCB-Y complexes, we examined in this study two types of DPCB-Y platinum complexes having π-donor ligands. First, a series of [Pt(tolan-X)(DPCB-Y)] complexes (**1–3**) were prepared in combination of each three kinds of *p*-substituents X and Y as listed in Table 1. The UV-vis absorption spectra exhibit clear dependence on substituents, which is consistent with the π-conjugation mediated by donor–acceptor interaction between tolan-X and DPCB-Y. Secondly, synthesis and structures of [Pt(dithiolato)(DPCB-Y)] complexes (**5** and **6**) were examined. Since dithiolates are known to be strong π-donor ligands,[11] we expected that donor–acceptor interaction may take place more efficiently than in tolan-X complexes.

Results and discussion

Synthesis and structures of alkyne complexes

Besides [Pt(tolan-X)(DPCB-phen)] (**4**) previously reported,[8] complexes **1–3** having three kinds of DPCB-Y ligands (Y = OMe, H, CF_3) were prepared from [Pt(cod)$_2$] by stepwise displacement of the cod ligands with tolan-X (1 equiv.) and then with DPCB-Y (1 equiv.) (Scheme 1).[12] Although ligand exchange reactions were examined in the opposite order, intermediate [Pt(cod)(DCPB-Y)] was poorly reactive, and an excess amount of tolan-X was required for the subsequent step.

Complexes **1–3** were identified by NMR spectroscopy and elemental analysis. Crystal structures of **2a**, **2c** and **3b** were examined by X-ray diffraction analysis. Fig. 2 shows the structure of **2a** as a representative example. The acetylenic carbons, platinum and diphosphinidenecyclobutene skeleton are in a planar arrangement; the dihedral angle between PtC(1)C(2) plane (**A**) and cyclobutene ring (**D**) is 2.2(1)°. On the other hand, the phenyl groups of tolan-H (**B** and **C**) are skewed from plane **A** by 26.0(1) and 9.3(1)°, respectively. The torsion angles are clearly larger than those observed for **4a** having the DPCB-Y ligand with a phenanthrene skeleton

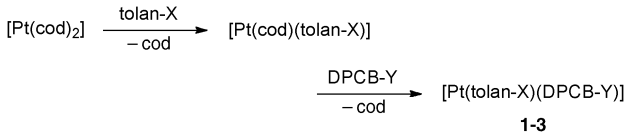

Scheme 1

(DPCB-phen), in which the benzene rings on the acetylenic carbons are tilted only by 7.6(1) and 5.3(1)° from the coordination plane. Complexes **2c** and **3b** exhibited the structural features similar to **2a**.

Table 2 compares the structural parameters of **2a**, **2c**, **3b** and **4a** with those of phosphine analogues.[13–16] The C(1)–C(2) lengths of DPCB-Y complexes range from 1.277(8) to 1.299(3) Å; the values are similar to those of phosphine analogues (1.280(5)–1.308(9) Å). The bent back angles of the phenyl groups of tolan-X against the C(1)–C(2) axis (*i.e.*, the α values in Table 2) are also in a comparable range. These structural parameters are known to reflect the efficiency of π-back donation from platinum to the in-plane π* orbital of tolan-X ($\pi_{\parallel}$: the π* orbital parallel to the coordination plane).[17] Furthermore, the π-back donation reflects the σ-donating ability of supporting ligands. Thus, the X-ray data indicate that DPCB-Y ligands are good σ-donors comparable to phosphines.

Table 3 summarizes the $^{13}C\{^1H\}$ NMR data for acetylenic carbons and the $^{31}P\{^1H\}$ NMR data for DPCB-Y ligands. The ^{13}C NMR signals appear at δ 121.5–125.4 with the $^1J_{PtC}$ values of 353–366 Hz. The chemical shift values are somewhat smaller than those of the tolan-H complexes with dppe and PPh_3 ligands (δ 135.6 and 127.1, respectively). An interesting phenomenon emerging from the ^{31}P NMR data is the upfield shift upon coordination. Thus the signals of **1–4** appear more clearly in an upper magnetic field than those of free DPCB-Y. This situation is opposite to that observed for dppe as a tertiary phosphine ligand, which exhibits a downfield shift

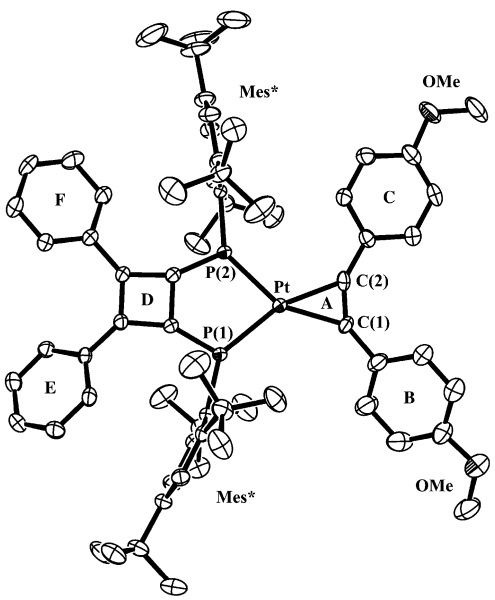

Fig. 2 ORTEP drawing of **2a** with the thermal ellipsoids at the 50% probability level. Hydrogen atoms are omitted for clarity.

Table 2 Selected bond distances (Å) and angles (°) for the X-ray structures of **2a**, **2c**, **3b** and related Pt(0) phosphine complexes

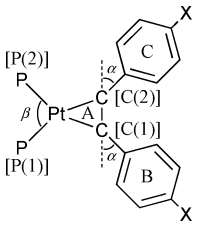

Compound	C(1)–C(2)	Pt–C(1), Pt–C(2)	Pt–P(1), Pt–P(2)	α	β	**A**–**B** dihedral	**A**–**C** dihedral
2a (X = OMe, Y = H)	1.297(5)	2.048(3), 2.027(3)	2.300(1), 2.2704(9)	36.7(4), 32.3(4)	82.96(3)	26.0(1)	9.3(1)
2c (X = CF_3, Y = H)	1.282(6)	2.034(4), 2.036(4)	2.279(1), 2.277(1)	30.2(4), 30.6(4)	82.79(4)	10.7(2)	8.7(2)
3b (X = H, Y = CF_3)	1.277(8)	2.050(5), 2.036(5)	2.266(2), 2.277(2)	30.7(5), 30.5(5)	82.97(6)	9.8(2)	14.1(2)
4a (X = OMe, Y = phen)	1.299(3)	2.053(2), 2.038(2)	2.3117(6), 2.2884(6)	28.3(2), 33.0(2)	82.95(5)	7.6(1)	5.3(1)
[Pt(tolan-H)(dppe)] (A)	1.284(9)	2.038(6), 2.039(6)	2.265(2), 2.267(2)	33.1(7), 35.7(6)	86.44(6)	31.1(3)	27.3(2)
[Pt(tolan-H)(dppe)] (B)	1.308(9)	2.029(6), 2.032(6)	2.262(2), 2.261(2)	35.6(7), 36.1(6)	86.35(6)	35.0(3)	31.6(3)
[Pt(tolan-H)(dppbz)]	1.301(4)	2.038(3), 2.041(3)	2.260(1), 2.266(1)	34.6(3), 33.6(3)	86.56(4)		
[Pt(tolan-H)(dppp)]	1.301(7)	2.041(3), 2.041(3)	2.2705(9), 2.2705(9)	35.5(2), 35.5(2)	96.02(5)		
[Pt(tolan-H)(PPh_3)$_2$]	1.280(5)	2.047(3), 2.048(3)	2.2910(8), 2.2820(9)	37.7(3), 37.4(3)	106.60(3)		

The dppe complex contains two independent molecules (A and B) in the crystal. dppe = 1,2-bis(diphenylphosphino)ethane, dppbz = 1,2-bis(diphenylphosphino)benzene, dppp = 1,3-bis(diphenylphosphino)propane.

upon coordination with platinum. There is a tendency that more electron-withdrawing tolan-X causes an upfield shift to a greater extent. As we discuss below for Pt(II) complexes, the extent of upfield shift is correlated with Pt–P lengths and thus with $^1J_{PtP}$ values. For example, in each series of tolan-X complexes with the same DPCB-Y ligand in Table 3, the ^{31}P NMR signal tends to be shifted upfield as the $^1J_{PtP}$ value increases. It was confirmed that the $^1J_{PtP}$ values exhibit a good Hammett correlation with the σ_p values[18] of substituent X (Fig. 3).

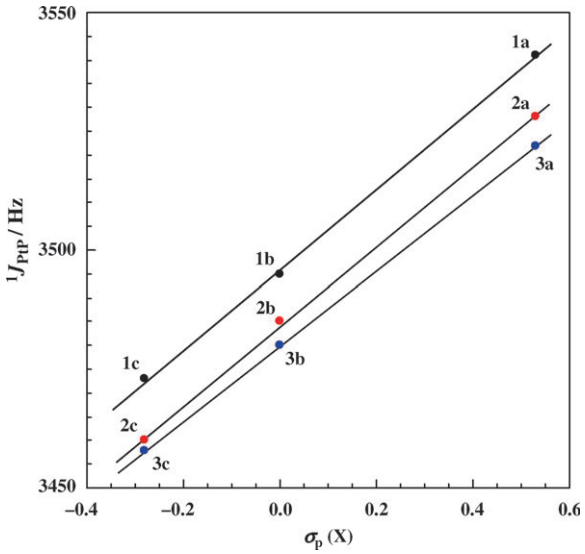

Fig. 3 Hammett plots for the substituent effects of tolan-X on the $^1J_{PtP}$ values of **1–3**.

Synthesis and structures of dithiolate complexes

DPCB-H and DPCB-phen complexes bearing 1,2-benzenedithiolato (bdt) and 1,3-dithia-2-thione-4,5-dithiolato (dmit) ligands were synthesized by anionic ligand exchange of [$PtCl_2$(DPCB-Y)] with thiolate sources (Scheme 2). The reactions with 1,2-benzenedithiol proceeded in THF in the presence 1,8-diazabicyclo[5.4.0]undec-7-ene (DBU) to give **5a** and **6a**, each in 72% yield, where slow addition of a large excess amount of DBU (> 50 equiv.) at low temperature (−78 °C) was essential to obtain the desired complexes in high yields, otherwise the reactions were not completed. On the other hand, [$PtCl_2$(DPCB-Y)] cleanly reacted with a stoichiometric amount of [NEt_4]$_2$[Zn(dmit)$_2$] in CH_2Cl_2 at room temperature to afford **5b** and **6b** in 92 and 77% yields, respectively.

Complexes **5** and **6** were identified by NMR spectroscopy and elemental analysis. The NMR data were fully consistent with C_{2v} symmetry of the complexes in solution, having a planar geometry except for Mes* groups on the phosphorus atoms. Thus, the two *ortho* *t*-Bu groups of the Mes* groups were observed equivalently in the ^{1}H and ^{13}C NMR spectra, showing orthogonal orientation of the Mes* groups against the coordination plane.

Fig. 4 shows the X-ray crystal structure of **5a**. In agreement with the NMR data, the complex adopts a significantly planar arrangement of the bdt, platinum and DPCB-H ligand with one twofold axis on the plane. The dihedral angle between the benzene ring of bdt (**A**) and the cyclobutene ring of DPCB-H ligand (**B**) is 1.8(1)°, whereas the phenyl groups of DPCB-H (**C** and **C**′) are twisted by 23.2(1)° against plane **B**. The latter value is notably smaller than that of free DPCB-H (40.0 and 42.6°).[7]

Table 4 compares the Pt–S and Pt–P lengths of **5a** with those of Pt(II) complexes having dimethyl,[7,19] dithiolato,[20–24] and dichloro ligands.[25,26] The Pt–S bonds of **5a** (2.2835(5) Å) are somewhat shorter than those of dppe and dppf complexes (2.308(1)–2.316(6) Å), but clearly longer than those of nitrogen-based ligand complexes (2.232(2)–2.251(4) Å). The Pt–P

Table 3 $^{13}C\{^1H\}$ and $^{31}P\{^1H\}$ NMR data for **1–4** and free DPCB-Y

Compound	$\delta_{C\equiv C}$	$^1J_{PtC}$	δ_P	$^1J_{PtP}$
DPCB-OMe	—	—	162.6	—
1a (X = OMe, Y = OMe)	121.6	353	153.0	3458
1b (X = H, Y = OMe)	123.9	366	152.6	3480
1c (X = CF_3, Y = OMe)	124.9	[a]	149.8	3522
DPCB-H	—	—	169.5	—
2a (X = OMe, Y = H)	121.8	361	160.0	3460
2b (X = H, Y = H)	124.0	365	159.7	3485
2c (X = CF_3, Y = H)	125.4	[a]	157.2	3528
DPCB-CF_3	—	—	180.7	—
3a (X = OMe, Y = CF_3)	122.1	362	169.6	3473
3b (X = H, Y = CF_3)	124.1	362	169.5	3495
3c (X = CF_3, Y = CF_3)	124.8	[a]	167.0	3541
DPCB-phen	—	—	173.2	—
4a (X = OMe, Y = phen)	121.5	358	156.6	3436
4b (X = H, Y = phen)	122.3	361	155.7	3455
dppe	—	—	–12.5	—
[Pt(tolan-H)(dppe)]	135.6	313	49.6	3110

The chemical shifts and coupling constants are given in ppm and Hz, respectively. The data were observed in CD_2Cl_2 at 20 °C.[a] The coupling constant was obscured due to broadening of the satellite signals.

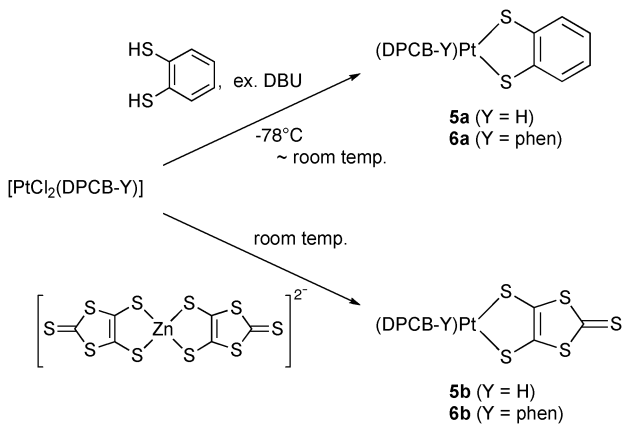

Scheme 2

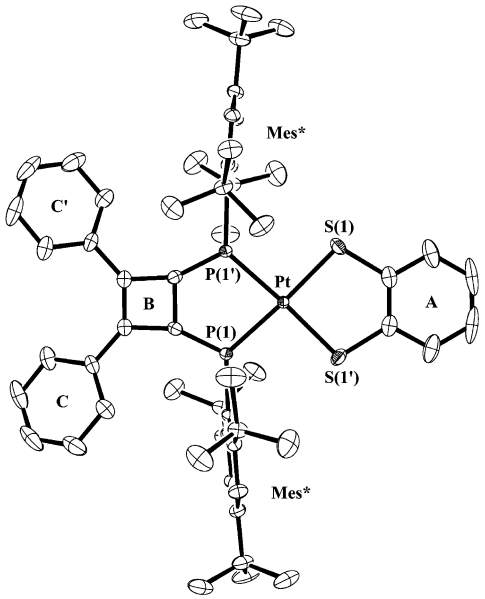

Fig. 4 ORTEP drawing of **5a** with the thermal ellipsoids at the 50% probability level. Hydrogen atoms are omitted for clarity. The atoms labeled with a prime character (′) are at (3/2 − x, 1 − y, z).

Table 4 Selected bond distances (Å) for the X-ray structures of **5a** and related Pt(II) complexes

Compound	Pt–S	Pt–P
[$PtMe_2$(DPCB-H)]	—	2.2909(8)
[Pt(bdt)(DPCB-H)] (**5a**)	2.2835(5)	2.2514(5)
[$PtCl_2$(DPCB-H)]	—	2.243(1), 2.245(1)
[$PtMe_2$(dppe)]	—	2.246(2), 2.254(2)
[Pt(bdt-NNtol)(dppe)]	2.310(1), 2.316(6)	2.260(9), 2.259(6)
[$PtCl_2$(dppe)]	—	2.208(6)
[Pt(bdt)(dppf)]	2.309(1), 2.308(1)	2.3126(7), 2.3298(9)
[Pt(bdt)(mesBIAN)]	2.232(2), 2.244(2)	—
[Pt(bdt)(bipy)]	2.244(2), 2.250(2)	—
[Pt(bdt-*t*-Bu_2)(phen-Ph_2)]	2.251(4), 2.244(4)	—

bdt = 1,2-benzenedithiolato, bdt-NNtol = 4-(tolylazo)benzene-1,2-dithiolato, mesBIAN = bis(mesityl)biazanaphthenequinone, bdt-*t*-Bu_2 = 3,5-di-*tert*-butylbenzene-1,2-dithiolato, phen-Ph_2 = 4,7-diphenyl-1,10-phenanthroline.

lengths are elongated as the *trans*-influence of diagonal ligands increases in the order Cl < bdt < Me.

Table 5 summarizes the ^{31}P NMR chemical shifts (δ_P), $^1J_{PtP}$ values, and averaged Pt–P bond lengths. It is seen from the data of DPCB-H complexes that $^1J_{PtP}$ values are proportional to Pt–P lengths as expected. Furthermore, δ_P values of DPCB-H and DPCB-phen complexes are in inverse proportion to $^1J_{PtP}$ values (Fig. 5). Thus, it is evident that δ_P values of DPCB-Y ligands are inversely proportional to Pt–P lengths. Although a similar tendency is observed for dppe complexes, the variation in chemical shifts is rather small.

As we described above, unlike dppe as a phosphine ligand, DPCB-Y ligands exhibit an upfield shift in the ^{31}P NMR spectra upon coordination. Dimethyl complexes with the longest Pt–P bonds exhibit almost the same δ_P values as free ligands. On the other hand, the signals of dichloro complexes with the shortest Pt–P bonds are shifted upfield by 40.6 (DPCB-H) and 49.9 ppm (DPCB-phen) compared with those of free DPCB-Y ligands, respectively. Since the chemical shifts of phosphorus atoms are principally controlled by the paramagnetic term, the linear dependence of the chemical shifts upon Pt–P distances will be useful for evaluating π-orbital interaction between DPCB-Y and platinum.

UV-vis absorption spectra of 1–3

Fig. 6 shows typical UV-vis absorption spectra of [Pt(tolan-X)(DPCB-Y)] (**1–3**). Schematic diagrams of important molecular orbitals are given in Fig. 7. Based on time-dependent DFT calculations (TD-DFT) for a model compound of **2b** having mesityl (Mes) groups in place of Mes*, three absorption bands marked I, II and III were identified. Band I is composed of several absorption bands, including a relatively large contribution of the HOMO(−1)/LUMO transition (23%).

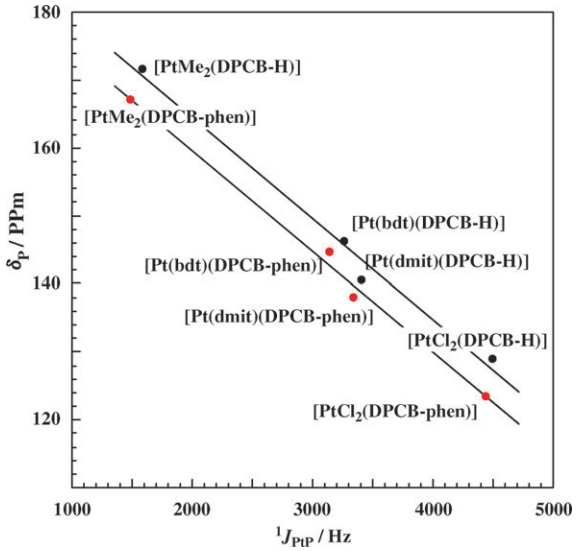

Fig. 5 Relation between ^{31}P NMR chemical shifts (δ_P) and coupling constants ($^1J_{PtP}$) for Pt(II) DPCB-Y complexes.

Table 5 $^{31}P\{^1H\}$ NMR data for Pt(II) complexes having DPCB-Y and dppe ligands

Compound	δ_P	$^1J_{PtP}$	Pt–P
DPCB-H	169.5	—	—
[$PtMe_2$(DPCB-H)]	171.6	1590	2.291
[Pt(bdt)(DPCB-H)] (**5a**)	146.1	3265	2.251
[Pt(dmit)(DPCB-H)] (**6a**)	140.4	3414	[a]
[$PtCl_2$(DPCB-H)]	128.9	4496	2.244
DPCB-phen	173.2	—	—
[$PtMe_2$(DPCB-phen)]	167.0	1489	[a]
[Pt(bdt)(DPCB-phen)] (**5b**)	144.7	3149	[a]
[Pt(dmit)(DPCB-phen) (**6b**)	138.0	3350	[a]
[$PtCl_2$(DPCB-phen)]	123.3	4444	[a]
dppe	−12.5	—	—
[$PtMe_2$(dppe)]	54.0	1783	2.250
[Pt(bdt-NNtol)(dppe)]	43.9	2775	2.260
[$PtCl_2$(dppe)]	43.8	3600	2.208

The data were observed in CD_2Cl_2 at 20 °C. The chemical shifts, coupling constants, and bond distances are given in ppm, Hz, and Å, respectively. The Pt–P length is the average of two bonds.[a] Not measured.

Band II includes major and minor contributions of the HOMO/LUMO(+1) (36%) HOMO(−1)/LUMO (11%) transitions, respectively. On the other hand, band III mainly consists of the HOMO/LUMO transition (45%), which is symmetry-forbidden, weak absorption.

Table 6 lists the absorption maxima (λ_{max}) of band I and band II, showing the effects of substituents X and Y on the absorption. Since all molecular orbitals participating in the absorption are π-symmetrical ones, no notable solvatochromic change in the absorption spectra was observed in cyclohexane, chloroform and acetone. The λ_{max} values are red-shifted as the electron-donating ability of X increases. This tendency is the one that is commonly observed for π-conjugated systems. On the other hand, the absorption tends to be shifted to the longer wavelengths as the electron-withdrawing nature of Y

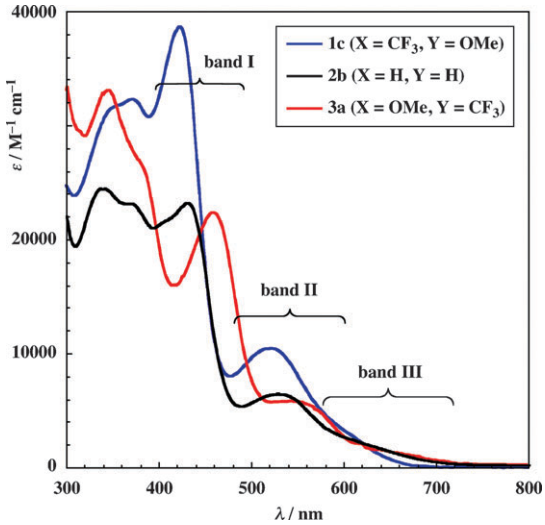

Fig. 6 Representative UV-vis absorption spectra of **1–3** in $CHCl_3$.

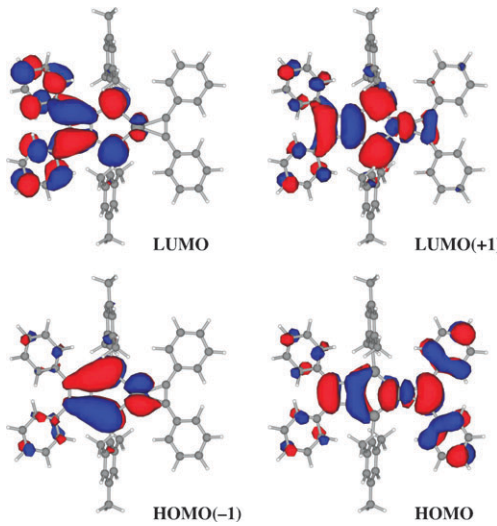

Fig. 7 Frontier orbitals of **2b** generated by DFT calculations for a model compound having Mes groups instead of Mes* groups.

increases. This tendency, which is most remarkable for band I of **3a–c** bearing a DPCB-CF_3 ligand, is opposite to the general observations on substituent effects. As we mentioned above, the absorption band I includes a relatively large contribution of the HOMO(−1)/LUMO transition, and the LUMO is mainly composed of the π orbital of DPCB-Y. Thus, it is reasonable that the CF_3 group results in a decrease in the LUMO level, and therefore causes the red shift in UV-vis absorption spectra. It is seen from Fig. 6 that this remarkable substituent effect of the CF_3 group as Y is of particular significance in **3a** with an electron-donating OMe group as X, showing the occurrence of donor–acceptor interaction between the tolan-X and DPCB-Y ligands.

UV-vis absorption spectra of 5 and 6

Fig. 8 compares UV-vis spectra of **6a** and **6b** with **4b**. Unlike **1–3** having DPCB-Y ligands (Y = OMe, H, CF_3), the DPCB-phen complexes display strong absorption bands in

Table 6 λ_{max} values (nm) for band I and band II of **1–3**

X (σ_p)	Y (σ_p)		
	OMe (−0.27)	H (0)	CF_3 (0.54)
Band I: λ_{max} (log ε)			
OMe (−0.27)	440 (4.29) (**1a**)	442 (4.38) (**2a**)	459 (4.34) (**3a**)
H (0)	430 (4.47) (**1b**)	432 (4.36) (**2b**)	448 (4.34) (**3b**)
CF_3 (0.54)	422 (4.58) (**1c**)	424 (4.53) (**2c**)	433 (4.53) (**3c**)
Band II: λ_{max} (log ε)			
OMe (–0.27)	542 (3.87) (**1a**)	545 (3.94) (**2a**)	548 (3.75) (**3a**)
H (0)	529 (3.95) (**1b**)	531 (3.80) (**2b**)	534 (3.61) (**3b**)
CF_3 (0.54)	519 (4.01) (**1c**)	519 (3.86) (**2c**)	521 (3.74) (**3c**)

The data were observed in $CHCl_3$ at room temperature.

the region of 500–700 nm. This is due to the reverse on the orbital levels between the LUMO and LUMO(+1). As seen from the orbital diagrams in Fig. 9, the orbital symmetry of the LUMO harmonizes with that of the HOMO, giving a symmetry-allowed transition with strong intensity. TD-DFT calculations for the models of **6a** and **6b** having Mes instead of Mes* revealed the absorption bands involving 37 and 41% contributions of the HOMO/LUMO transition, respectively. Recently, related platinum dithiolates supported by nitrogen-based ligands were reported to exhibit strong MLCT bands in a similar region with remarkable solvatochromism.[22] On the other hand, the present DPCB-phen complexes were insensitive to solvent polarity among chloroform, THF and acetone. Therefore, in conjunction with the orbital distribution found in Fig. 9, the HOMO/LUMO transition of DPCB-phen complexes are assigned to π–π* transition.

Table 7 lists the data for lowest-energy absorption of **5** and **6**. Complexes **5a** and **6a** with a 1,2-benzenedithiolato ligand (bdt) exhibit the λ_{max} values of 556 and 583 nm, respectively. These values are red-shifted by 12 and 21 nm, respectively, when the bdt ligand is replaced by 1,3-dithia-2-thione-4,5-dithiolato (dmit) as a stronger π-donor than bdt. As judging from the values of absorption maxima and HOMO–LUMO gaps (HLG), the combination of dmit and DPCB-phen ligands

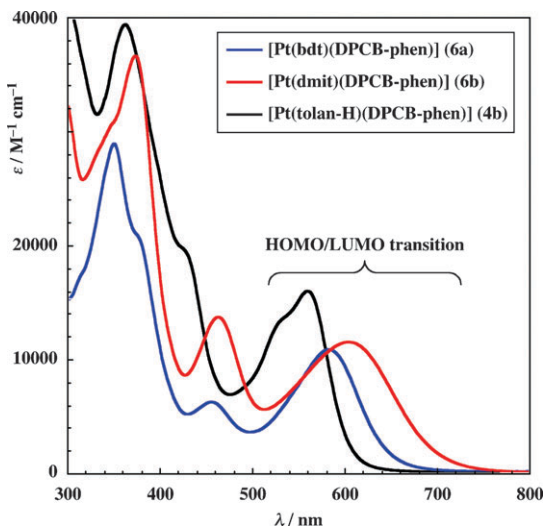

Fig. 8 UV-vis absorption spectra for **6a**, **6b** and **4b** in $CHCl_3$.

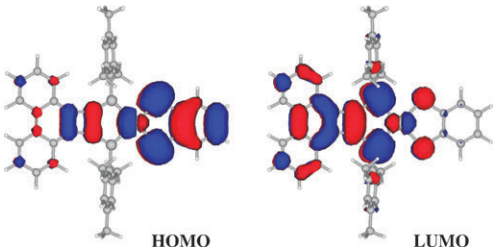

Fig. 9 Frontier orbitals of **6a** generated by DFT calculations for a model compound having Mes groups instead of Mes* groups.

is particular effective for enhancement in the extended π-conjugation within the molecule. The HLG value of **6b** (1.77 eV) was clearly lower than those of **4a** (2.06 eV) and **4b** (1.99 eV), and comparable to that of [Pt(tolan-NMe_2)-(DPCB-phen)] having strongly electron-donating NMe_2 groups on the tolan-X ligand (1.82 eV).[8]

Conclusions

The DPCB-Y complexes of platinum possess rather unique electronic properties, clearly different from diphosphine and diimine analogues. Most of them are rationalized by assuming the occurrence of dπ–pπ interaction between the DPCB-Y ligands and platinum. Thus, the ^{31}P NMR chemical shifts are highly sensitive to Pt–P distances, and linearly correlated with the bond lengths. Moreover, the complexes exhibit the absorption bands at significantly longer wavelengths. Unlike the diimine complexes showing a MLCT band, these absorptions are assignable to π–π* transitions derived from extended π-conjugation within the molecules. Further applications of these unique ligand properties to organometallic chemistry will be reported in due course.

Experimental

All manipulations were performed under a nitrogen or argon atmosphere using standard Schlenk techniques. NMR spectra were recorded on a Bruker AVANCHE 400 spectrometer (^1H, 400.13 MHz; ^{13}C, 100.62 MHz; ^{31}P, 161.98 MHz). Chemical shifts are reported in δ, referenced to ^1H (of residual protons) and ^{13}C signals of deuterated solvents as internal standards or to the ^{31}P signal of 85% H_3PO_4 as an external standard. UV-vis absorption spectra were measured on a JASCO V550 spectrometer. Elemental analysis was performed by the ICR Analytical Laboratory, Kyoto University.

Synthetic procedures for DPCB-Y ligands were previously reported.[7,27] $[Pt(cod)_2]$ and $[Et_4N]_2[Zn(dmit)_2]$ were prepared according to the literature.[28,29] $[PtCl_2(DPCB\text{-}H)]$ and

Table 7 Lowest-energy absorption data for **5** and **6**

Compound	λ_{max} (log ε)	λ_{edge}	HLG
[Pt(bdt)(DPCB-H)] (**5a**)	556 (3.76)	636	1.94
[Pt(dmit)(DPCB-H)] (**5b**)	568 (3.85)	674	1.83
[Pt(bdt)(DPCB-phen)] (**6a**)	583 (4.03)	646	1.91
[Pt(dmit)(DPCB-phen) (**6b**)	604 (4.06)	701	1.77

The data were obtained in $CHCl_3$ at room temperature. The HLG values were estimated from the absorption edge wavelengths (λ_{edge}).

[$PtCl_2$(DPCB-phen)] were obtained by ligand displacement of [$PtCl_2$(cod)] and [$PtCl_2(SMe_2)_2$] with the corresponding DPCB-Y ligand, respectively. Other chemicals were obtained from commercial sources and used as received.

Synthesis

[Pt(tolan-X)(DPCB-Y)] (X = OMe, H). A typical procedure is reported for **2a** (X = OMe, Y = H). The complex [Pt(cod)$_2$] (419 mg, 1.02 mmol) was suspended in hexane (13 mL) at −20 °C, and a solution of 1,2-bis(4-methoxyphenyl)ethyne (tolan-OMe) (243 mg, 1.02 mmol) in Et_2O (6 mL) was added dropwise with stirring. After 1 h, a pale yellow precipitate of [Pt(tolan-OMe)(cod)] formed in the system was collected by filtration, washed with hexane (5 mL × 3), and dried under vacuum (415 mg, 75%).

A part of the product (124 mg, 0.229 mmol) was dissolved in CH_2Cl_2 (3 mL), and solid DPCB (173 mg, 0.229 mmol) was added in one portion. The mixture was stirred for 2 h at room temperature, and then concentrated to dryness. The resulting solid was washed with hexane (2 mL × 3) and dried under vacuum to afford deep purple powder of **2a** (153 mg, 56%), which was analytically pure. The product was dissolved in CH_2Cl_2 (*ca.* 0.5 mL), layered with MeOH (2 mL), and allowed to stand at room temperature to give single crystals suitable for X-ray diffraction analysis.

Complexes **1a** (64%), **1b** (60%), **2b** (70%), **3a** (46%) and **3b** (27%) were similarly prepared and characterized by NMR spectroscopy and elemental analysis.

1a (X = OMe, Y = OMe). ^{1}H NMR (CD_2Cl_2, 20 °C): δ 1.51 (s, 18H), 1.66 (s, 36H), 3.72 (s, 6H), 3.76 (s, 6H), 6.47 (d, J = 9.0 Hz, 4H), 6.67 (d, J = 9.0 Hz, 4H), 6.87 (d, J = 9.0 Hz, 4H), 7.61 (d, J = 8.7 Hz, 4H), 7.66 (s, 4H). ^{13}C{^{1}H} NMR (CD_2Cl_2, 20 °C): δ 31.7 (s), 33.8 (s), 35.7 (s), 39.4 (s), 55.5 (s), 113.6 (s), 113.9 (s), 121.6 (m, J_{PtC} = 353 Hz, C≡C), 123.2 (s), 124.2 (t, J_{PC} = 11 Hz), 125.0 (s), 129.4 (s), 132.6 (s, J_{PtC} = 160 Hz), 133.3 (t, J_{PC} = 3 Hz, J_{PtC} = 54 Hz), 146.4 (t, J_{PC} = 9 Hz), 152.6 (s), 156.2 (s), 158.8 (s), 160.0 (s), 172.8 (dd, J_{PC} = 33 and 31 Hz). ^{31}P{^{1}H} NMR (CD_2Cl_2, 20 °C): δ 153.0 (s, J_{PtP} = 3458 Hz). Anal. calcd for $C_{70}H_{86}O_4P_2Pt$: C, 67.34; H, 6.94%. Found: C, 67.02; H, 6.97%.

2a (X = OMe, Y = H). ^{1}H NMR (CD_2Cl_2, 20 °C): δ 1.48 (s, 18H), 1.63 (s, 36H), 3.75 (s, 6H), 6.66 (d, J = 9.0 Hz, 4H), 6.91–6.95 (m, 8H), 7.10–7.15 (m, 2H), 7.60 (d, J = 9.0 Hz, 4H), 7.63 (s, 4H). ^{13}C{^{1}H} NMR (CD_2Cl_2, 20 °C): δ 31.6 (s), 33.9 (s), 35.7 (s), 39.4 (s), 55.5 (s), 113.6 (s), 121.8 (m, J_{PtC} = 361 Hz, C≡C), 123.3 (s), 124.0 (t, J_{PC} = 11 Hz), 127.7 (s), 128.5 (s), 128.7 (s), 132.2 (s, J_{PtC} = 160 Hz), 132.3 (s), 133.4 (t, J_{PC} = 4 Hz, J_{PtC} = 54 Hz), 147.4 (t, J_{PC} = 9 Hz), 152.8 (s), 156.1 (s), 158.9 (s) 172.2 (dd, J_{PC} = 32 and 31 Hz). ^{31}P{^{1}H} NMR (CD_2Cl_2, 20 °C): δ 160.0 (s, J_{PtP} = 3460 Hz). Anal. calcd for $C_{68}H_{82}O_2P_2Pt$: C, 68.73; H, 6.96%. Found: C, 68.40; H, 6.94%.

3a (X = OMe, Y = CF_3). ^{1}H NMR (CD_2Cl_2, 20 °C): δ 1.48 (s, 18H), 1.62 (s, 36H), 3.76 (s, 6H), 6.68 (d, J = 8.4 Hz, 4H), 6.97 (d, J = 8.1 Hz, 4H), 7.17 (d, J = 8.1 Hz, 4H), 7.60 (d, J = 8.7 Hz, 4H), 7.63 (s, 4H). ^{13}C{^{1}H} NMR (CD_2Cl_2, 20 °C): δ 31.6 (s), 34.0 (s), 35.7 (s), 39.4 (s), 55.5 (s), 113.7 (s), 122.1 (m, J_{PtC} = 362 Hz, C≡C), 123.6 (s), 123.7 (t, J_{PC} = 11 Hz), 124.5 (q, J_{FC} = 272 Hz), 125.6 (d, J_{PC} = 6 Hz), 127.7 (s), 129.9 (q, J_{FC} = 32 Hz), 131.7 (s, J_{PtC} = 160 Hz), 133.4 (t, J_{PC} = 4 Hz, J_{PtC} = 54 Hz), 135.7 (s), 146.1 (t, J_{PC} = 10 Hz), 153.3 (s), 156.3 (s), 159.2 (s), 171.0 (t, J_{PC} = 32 Hz). ^{31}P{^{1}H} NMR (CD_2Cl_2, 20 °C): δ 169.6 (s, J_{PtP} = 3473 Hz). Anal. calcd for $C_{70}H_{80}F_6O_2P_2Pt$: C, 63.48; H, 6.09%. Found: C, 63.28; H, 6.09%.

1b (X = H, Y = OMe). ^{1}H NMR (CD_2Cl_2, 20 °C): δ 1.50 (s, 18H), 1.64 (s, 36H), 3.71 (s, 6H), 6.45 (d, J = 9.0 Hz, 4H), 6.85 (d, J = 8.7 Hz, 4H), 7.12 (d, J = 1.8 Hz, 4H), 7.14 (s, 2H), 7.64 (s, 4H), 7.67 (dd, J = 7.2 and 1.5 Hz, 4H). ^{13}C{^{1}H} NMR (CD_2Cl_2, 20 °C): δ 31.7 (s), 33.5 (s), 35.7 (s), 39.4 (s), 55.5 (s), 113.9 (s), 123.2 (s), 123.9 (s, J_{PtC} = 366 Hz, C≡C), 124.8 (s), 126.9 (s), 128.3 (s), 129.4 (s), 131.6 (t, J_{PC} = 11 Hz), 131.8 (t, J_{PC} = 4 Hz, J_{PtC} = 52 Hz), 132.3 (s, J_{PtC} = 160 Hz), 146.6 (t, J_{PC} = 9 Hz), 152.7 (s), 156.3 (s), 160.1 (s), 173.1 (dd, J_{PC} = 32 and 31 Hz). ^{31}P{^{1}H} NMR (CD_2Cl_2, 20 °C): δ 152.6 (s, J_{PtP} = 3480 Hz). Anal. calcd for $C_{68}H_{82}O_2P_2Pt$: C, 68.73; H, 6.96%. Found: C, 68.43; H, 6.97%.

2b (X = H, Y = H). ^{1}H NMR (CD_2Cl_2, 20 °C): δ 1.51 (s, 18H), 1.66 (s, 36H), 6.95 (d, J = 4.5 Hz, 8H), 7.14–7.17 (m, 8H), 7.65 (s, 4H), 7.69 (dd, J_{HH} = 7.8 and 2.7 Hz, 4H). ^{13}C{^{1}H} NMR (CD_2Cl_2, 20 °C): δ 31.7 (s), 33.9 (s), 35.7 (s), 39.4 (s), 123.3 (s), 124.0 (m, J_{PtC} = 365 Hz, C≡C), 127.0 (s), 127.7 (s), 128.3 (s), 128.6 (s), 128.8 (s), 131.5 (t, J_{PC} = 10 Hz), 131.8 (t, J_{PC} = 4 Hz, J_{PtC} = 52 Hz), 131.9 (s, J_{PtC} = 160 Hz), 132.3 (s), 147.6 (t, J_{PC} = 9 Hz), 152.9 (s), 156.2 (s), 172.6 (dd, J_{PC} = 32 and 31 Hz). ^{31}P{^{1}H} NMR (CD_2Cl_2, 20 °C): δ 159.7 (s, J_{PtP} = 3485 Hz). Anal. calcd for $C_{66}H_{78}P_2Pt$: C, 70.25; H, 6.97%. Found: C, 70.45; H, 6.90%.

3b (X = H, Y = CF_3). ^{1}H NMR (CD_2Cl_2, 20 °C): δ 1.53 (s, 18H), 1.68 (s, 36H), 7.02 (d, J = 8.4 Hz, 4H), 7.17–7.25 (m, 10H), 7.69 (s, 4H), 7.74 (dd, J = 7.8 and 2.1 Hz, 4H). ^{13}C{^{1}H} NMR (CD_2Cl_2, 20 °C): δ 31.6 (s), 34.0 (s), 35.7 (s), 39.4 (s), 123.6 (s), 124.1 (m, J_{PtC} = 362 Hz, C≡C), 124.5 (q, J_{FC} = 273 Hz), 125.7 (d, J_{PC} = 4 Hz), 127.4 (s), 127.7 (s), 128.4 (s), 129.9 (q, J_{FC} = 32 Hz), 131.2 (t, J_{PC} = 10 Hz), 131.4 (s, J_{PtC} = 160 Hz), 131.9 (t, J_{PC} = 4 Hz, J_{PtC} = 51 Hz), 135.6 (s), 146.2 (t, J_{PC} = 10 Hz), 153.4 (s), 156.4 (s), 171.4 (dd, J_{PC} = 32 and 31 Hz). ^{31}P{^{1}H} NMR (CD_2Cl_2, 20 °C): δ 169.5 (s, J_{PtP} = 3495 Hz). Anal. calcd for $C_{68}H_{76}F_6P_2Pt$: C, 64.60; H, 6.06%. Found: C, 64.80; H, 6.05%.

[Pt(tolan-CF_3)(DPCB-Y)]. A typical procedure is reported for **2c** (Y = H). The complex [Pt(cod)$_2$] (23 mg, 0.056 mmol) was dissolved in CH_2Cl_2 (2 mL) at room temperature, and 1,2-bis(4-trifluoromethylphenyl)ethyne (tolan-CF_3) (18 mg, 0.057 mmol) was added with stirring. After 5 min, DPCB (43 mg, 0.057 mmol) was added, and the mixture was stirred for additional 2 h. Volatile substances were removed under reduced pressure, and the residue was washed with hexane (2 mL × 3) and dried under vacuum to give **2c** as dark red powder (32 mg, 45%). Complexes **1c** (59%) and **3c** (30%) were similarly prepared.

1c (X = CF_3, Y = OMe). ^{1}H NMR (CD_2Cl_2, 20 °C): δ 1.53 (s, 18H), 1.66 (s, 36H), 3.74 (s, 6H), 6.49 (d, J = 9.0 Hz, 4H), 6.90 (d, J = 9.0 Hz, 4H), 7.42 (d, J = 8.4 Hz, 4H), 7.68 (s,

4H), 7.76 (d, J = 7.8 Hz, 4H). $^{13}C\{^1H\}$ NMR (CD_2Cl_2, 20 °C): δ 31.7 (s), 33.9 (s), 35.8 (s), 39.4 (s), 55.6 (s), 114.1 (s), 123.5 (s), 124.6 (s), 124.9 (q, J_{FC} = 272 Hz), 124.9 (m, C≡C), 125.4 (d, J_{PC} = 3 Hz), 128.3 (q, J_{FC} = 32 Hz), 129.6 (s), 131.5 (t, J_{PC} = 3 Hz, J_{PtC} = 54 Hz), 131.6 (s, J_{PtC} = 159 Hz), 135.4 (t, J_{PC} = 11 Hz), 147.2 (t, J_{PC} = 9 Hz), 153.2 (s), 156.5 (s), 160.4 (s) 173.6 (dd, J_{PC} = 33 and 31 Hz). $^{31}P\{^1H\}$ NMR (CD_2Cl_2, 20 °C): δ 149.8 (s, J_{PtP} = 3522 Hz). Anal. calcd for $C_{70}H_{80}F_6O_2P_2Pt$: C, 63.48; H, 6.09%. Found: C, 63.84; H, 5.85%.

2c (X = CF_3, Y = H). ^1H NMR (CD_2Cl_2, 20 °C): δ 1.49 (s, 18H), 1.63 (s, 36H), 6.94–6.99 (m, 8H), 7.13–7.19 (m, 2H), 7.40 (d, J = 8.1 Hz, 4H), 7.64 (s, 4H), 7.73 (d, J = 8.1 Hz, 4H). $^{13}C\{^1H\}$ NMR (CD_2Cl_2, 20 °C): δ 31.6 (s), 33.9 (s), 35.7 (s), 39.4 (s), 123.5 (s), 124.8 (q, J_{FC} = 272 Hz), 125.4 (m, C≡C), 125.4 (d, J_{PC} = 3 Hz), 127.8 (s), 128.4 (q, J_{FC} = 32 Hz), 128.6 (s), 129.2 (s), 131.1 (s, J_{PtC} = 158 Hz), 131.5 (t, J_{PC} = 3 Hz, J_{PtC} = 52 Hz), 131.9 (s), 135.3 (t, J_{PC} = 12 Hz), 148.2 (t, J_{PC} = 10 Hz), 153.3 (s), 156.3 (s), 173.0 (dd, J_{PC} = 33 and 31 Hz). $^{31}P\{^1H\}$ NMR (CD_2Cl_2, 20 °C): δ 157.2 (s, J_{PtP} = 3528 Hz). Anal. calcd for $C_{68}H_{76}F_6P_2Pt$: C, 64.60; H, 6.06%. Found: C, 64.55; H, 6.15%.

3c (X = CF_3, Y = CF_3). ^1H NMR (CD_2Cl_2, 20 °C): δ 1.49 (s, 18H), 1.63 (s, 36H), 6.99 (d, J = 8.1 Hz, 4H), 7.21 (d, J = 8.4 Hz, 4H), 7.44 (d, J = 8.1 Hz, 4H), 7.66 (s, 4H), 7.74 (d, J = 7.8 Hz, 4H). $^{13}C\{^1H\}$ NMR (CD_2Cl_2, 20 °C): δ 31.6 (s), 34.0 (s), 35.8 (s), 39.4 (s), 123.7 (s), 124.4 (q, J_{FC} = 272 Hz), 124.8 (q, J_{FC} = 272 Hz), 124.8 (m, C≡C), 125.5 (d, J_{PC} = 3 Hz), 125.7 (d, J_{PC} = 3 Hz), 127.8 (s), 128.7 (q, J_{FC} = 32 Hz), 130.3 (q, J_{FC} = 33 Hz), 130.5 (s, J_{PtC} = 159 Hz), 131.5 (t, J_{PC} = 4 Hz, J_{PtC} = 50 Hz), 135.0 (t, J_{PC} = 10 Hz), 135.3 (s), 146.7 (t, J_{PC} = 10 Hz), 153.8 (s), 156.5 (s), 171.7 (dd, J_{PC} = 33 and 31 Hz). $^{31}P\{^1H\}$ NMR (CD_2Cl_2, 20 °C): δ 167.0 (s, J_{PtP} = 3541 Hz). Anal. calcd for $C_{70}H_{74}F_{12}P_2Pt$: C, 60.04; H, 5.33%. Found: C, 59.64; H, 5.56%.

[Pt(tolan-H)(dppe)]. To a solution of [Pt(tolan)(cod)] (33 mg, 0.069 mmol) in CH_2Cl_2 (2 mL) was added 1,2-bis(diphenylphosphanyl)ethane (dppe) (28 mg, 0.070 mmol) at −30 °C with stirring. After 1 h, the solvent was removed under reduced pressure. The residue was dissolved in CH_2Cl_2 (*ca.* 0.5 mL), layered with Et_2O (2 mL), and allowed to stand at 0 °C, giving pale yellow crystals of the title compound (42 mg, 79%). ^1H NMR (CD_2Cl_2, 20 °C): δ 2.38 (dt, J = 14.4 and 9.6 Hz, 4H), 7.14 (d, J = 7.2 Hz, 2H), 7.20 (dd, J = 6.9 and 7.2 Hz, 4H), 7.32–7.40 (m, 4H), 7.64 (dd, J = 8.4 and 1.5 Hz, 4H), 7.76–7.83 (m, 8H). $^{13}C\{^1H\}$ NMR (CD_2Cl_2, 20 °C): δ 31.1 (dd, J_{PC} = 10 Hz, J_{PtC} = 50 Hz), 126.4 (s), 128.5 (s), 128.8 (t, J_{PC} = 7 Hz), 130.4 (s), 130.8 (t, J_{PC} = 3 Hz, J_{PtC} = 43 Hz), 133.3 (t, J_{PC} = 8 Hz, J_{PtC} = 25 Hz), 135.3 (t, J_{PC} = 22 Hz), 135.8 (t, J_{PC} = 9 Hz), 135.6 (m, J_{PtC} = 313 Hz, C≡C). $^{31}P\{^1H\}$ NMR (CD_2Cl_2, 20 °C): δ 49.6 (s, J_{PtC} = 3110 Hz).

[Pt(bdt)(DPCB-Y)]. To a solution of [$PtCl_2$(DPCB-H)] (50 mg, 0.049 mmol) and 1,2-benzenedithiol (10 mg, 0.074 mmol) in THF (2.5 mL) was added dropwise DBU (450 mg, 2.94 mmol) at −78 °C. The reaction mixture was gradually warmed to room temperature and stirred for 2 h to give a dark green solution. After removal of volatiles under reduced pressure, the residue was washed with Et_2O at −78 °C and dried under vacuum. Crystallization of the resulting compound from a CH_2Cl_2–Et_2O mixed solvent gave **5a** as dark red crystals (38 mg, 72%). Complex **6a** was similarly prepared in 72% yield.

5a (Y = H). ^1H NMR (CD_2Cl_2, 20 °C): δ 1.41 (s, 18H), 1.67 (s, 36H), 6.75 (t, J = 3.2 Hz, 2H), 6.87–6.88 (m, 8H) 7.14 (dd, J = 4.4 and 4.0 Hz, 2H), 7.42 (t, J = 3.2 Hz, 2H), 7.64 (4H, d, J = 2.8 Hz). $^{13}C\{^1H\}$ NMR (CD_2Cl_2, 20 °C): δ 31.6 (s), 35.4 (s), 36.0 (s), 40.2 (s), 122.4 (s), 123.5 (d, J_{PC} = 20 Hz), 124.9 (dd, J_{PC} = 5 Hz), 128.0 (s), 128.6 (s), 129.0 (s), 130.5 (s), 131.1 (s), 144.9 (t, J_{PC} = 6 Hz), 149.3 (dd, J_{PC} = 49 and 32 Hz), 155.4 (s), 158.2 (s), 166.9 (dd, J_{PC} = 68 and 18 Hz). $^{31}P\{^1H\}$ NMR (CD_2Cl_2, 20 °C): δ 146.1 (s, J_{PtP} = 3265 Hz). Anal. calcd for $C_{58}H_{72}P_2PtS_2$: C, 63.89; H, 6.66%. Found: C, 63.46; H, 6.67%.

6a (Y = phen): ^1H NMR (CD_2Cl_2, 20 °C): δ 1.50 (s, 18H), 1.75 (s, 36H), 6.17 (d, J = 8.0 Hz, 2H), 6.75 (t, J = 3.2 Hz, 2H), 7.24 (dd, J = 7.6 and 8.0 Hz, 2H), 7.42 (t, J = 3.2 Hz, 2H), 7.63 (dd, J = 7.6 and 8.4 Hz, 2H), 7.78 (s, 4H), 8.54 (d, J = 8.4 Hz, 2H). $^{13}C\{^1H\}$ NMR (CD_2Cl_2, 20 °C): δ 31.7 (s), 35.4 (s), 36.1 (s), 40.0 (s), 122.6 (s), 123.7 (d, J_{PC} = 14 Hz), 124.3 (s), 124.4 (s), 124.7 (s), 125.7 (s), 128.4 (s), 128.6 (s), 129.3 (s), 133.2 (t, J_{PC} = 3 Hz), 144.6 (dd, J_{PC} = 57 and 21 Hz), 155.6 (s), 159.2 (s), 168.4 (dd, J_{PC} = 62 and 21 Hz). $^{31}P\{^1H\}$ NMR (CD_2Cl_2, 20 °C): δ 144.7 (s, J_{PtP} = 3149 Hz). Anal. calcd for $C_{58}H_{70}P_2PtS_2$: C, 64.41; H, 6.48%. Found: C, 63.79; H, 6.35%.

[Pt(dmit)(DPCB-Y)]. To a 10 ml Schlenk tube were added [$PtCl_2$(DPCB-H)] (50 mg, 0.049 mmol), [NEt_4]$_2$[Zn(dmit)$_2$] (19 mg, 0.027 mmol), and CH_2Cl_2 (2.5 mL). The solution was stirred overnight at room temperature, and washed with brine (2 mL × 3) and H_2O (2 mL × 1). The organic phase was dried over Na_2SO_4 and concentrated to dryness under vacuum. The residue was washed with acetone to afford **5b** as a dark green powder (52 mg, 92%). Complex **6b** was similarly synthesized in 77% yield.

5b (Y = H): ^1H NMR (CD_2Cl_2, 20 °C): δ 1.46 (s, 18H), 1.69 (s, 36H), 6.95–6.99 (m, 8H), 7.24 (dd, J = 4.4 and 4.0 Hz, 2H), 7.74 (d, J = 3.2 Hz, 4H). $^{13}C\{^1H\}$ NMR (CD_2Cl_2, 20 °C): δ 31.5 (s), 35.5 (s), 36.0 (s), 40.2 (s), 122.1 (d, J_{PC} = 40 Hz), 125.2 (s), 128.2 (s), 129.1 (s), 130.5 (s), 131.0 (s), 136.2 (t, J_{PC} = 9 Hz), 149.9 (t, J_{PC} = 61 Hz), 156.0 (s), 158.1 (s), 166.2 (t, J_{PC} = 37 Hz), 222.3 (s). $^{31}P\{^1H\}$ NMR (CD_2Cl_2, 20 °C): δ 140.4 (s, J_{PtP} = 3414 Hz). Anal. calcd for $C_{55}H_{68}P_2PtS_5$: C, 57.62; H, 5.98%. Found: C, 57.55; H, 5.99%.

6b (Y = phen). ^1H NMR (CD_2Cl_2, 20 °C): δ 1.50 (s, 18H), 1.73 (s, 36H), 6.25 (d, J = 8.0 Hz, 2H), 7.24 (dd, J = 7.6 and 8.0 Hz, 2H), 7.62 (dd, J = 7.6 and 8.4 Hz, 2H), 7.81 (d, J = 4.0 Hz, 4H), 8.54 (d, J = 8.4 Hz, 2H). $^{13}C\{^1H\}$ NMR (CD_2Cl_2, 20 °C): δ 31.6 (s), 35.4 (s), 36.1 (s), 40.0 (s), 122.4 (d, J_{PC} = 40 Hz), 124.4 (s), 124.5 (s), 124.8 (s), 125.7 (s), 128.8 (s), 129.9 (s), 133.5 (t, J_{PC} = 6 Hz), 144.0 (t, J_{PC} = 56 Hz), 156.2 (s), 159.2 (s), 167.7 (dd, J_{PC} = 48 and 50 Hz), 222.5 (s). $^{31}P\{^1H\}$ NMR (CD_2Cl_2, 20 °C): δ 138.0 (s, J_{PtP} = 3350 Hz). Anal. calcd for $C_{55}H_{66}P_2PtS_5$: C, 57.72; H, 5.81%. Found: C, 57.66; H, 5.85%.

Table 8 Crystallographic data for **2a**, **2c**, **3b**, **5a**, [Pt(tolan-H)(dppe)], and [$PtCl_2$(DPCB-H)]

Compound	**2a**	**2c**	**3b**	**5a**	[Pt(tolan-H)(dppe)]	[$PtCl_2$(DPCB-H)]·Me_2CO
Formula	$C_{68}H_{82}O_2P_2Pt$	$C_{68}H_{76}F_6P_2Pt$	$C_{68}H_{76}F_6P_2Pt$	$C_{58}H_{72}P_2Pt_1S_2$	$C_{40}H_{34}P_2Pt$	$C_{52}H_{68}Cl_2P_2Pt{\cdot}C_3H_6O$
Formula weight	1188.37	1264.32	1264.32	1090.31	771.70	1079.07
Space group	$P\bar{1}$	$P\bar{1}$	$P\bar{1}$	*Pnca*	$P\bar{1}$	$P2_1/c$
a/Å	9.264(2)	9.164(3)	9.477(4)	15.746(2)	10.8407(10)	19.008(9)
b/Å	16.459(4)	16.791(5)	11.489(5)	16.859(2)	17.0681(18)	14.477(4)
c/Å	20.290(5)	21.506(7)	29.035(13)	19.937	19.0121(17)	19.693(6)
α (°)	97.529(5)	70.738(8)	86.858(15)	90.00	79.591(6)	90.00
β (°)	91.894(5)	82.039(12)	88.386(15)	90.00	73.981(6)	111.193(4)
γ (°)	91.270(5)	87.536(12)	80.386(14)	90.00	85.655(6)	90.00
V/Å^3	3064.2(12)	3093.9(17)	3112(2)	5292.3(12)	3324.3(6)	5053(3)
Z	2	2	2	4	4	4
μ(Mo-Kα)/mm^{-1}	2.384	2.376	2.362	2.826	4.344	2.983
T/K	173(2)	173(2)	173(2)	173(2)	295(2)	203(2)
Reflections collected	24595	25002	25137	40678	32907	47646
Unique reflections	13360 (R_{int} = 0.0311)	13521 (R_{int} = 0.0375)	13606 (R_{int} = 0.0538)	6007 (R_{int} = 0.0498)	14900 (R_{int} = 0.0351)	14549 (R_{int} = 0.0587)
GOF	1.040	1.078	1.088	0.627	1.086	1.056
R indices	R_1 = 0.0354	R_1 = 0.0454	R_1 = 0.0554	R_1 = 0.0232	R_1 = 0.0564	R_1 = 0.0485
($I > 2\sigma(I)$)	wR_2 = 0.0831	wR_2 = 0.0964	wR_2 = 0.1253	wR_2 = 0.0780	wR_2 = 0.1292	wR_2 = 0.1454
R indices	R_1 = 0.0444	R_1 = 0.0530	R_1 = 0.0707	R_1 = 0.0287	R_1 = 0.0833	R_1 = 0.0524
(All data)	wR_2 = 0.0886	wR_2 = 0.1012	wR_2 = 0.1371	wR_2 = 0.0848	wR_2 = 0.1411	wR_2 = 0.1499

The space group "*Pnca*" for **5a** is a non-standard setting of space group "*Pbcn*".

X-Ray diffraction analysis

The X-ray diffraction studies were performed on a Rigaku Mercury CCD diffractometer with graphite-monochromated Mo-Kα radiation (λ = 0.71070 Å). The intensity data were collected at 173, 203, or 295 K, and corrected for Lorentz and polarization effects and absorption (numerical). The structure was solved by direct methods (SHELXS-97) and refined on F^2 for all reflections (SHELXL-97).[30] The crystallographic data and the summary of solution and refinement are listed in Table 8. CCDC reference numbers 735887 and 765285–765289. For crystallographic data in CIF or other electronic format see DOI: 10.1039/c0nj00118j

Computational studies

All calculations were performed with the Gaussian 03 program using the B3LYP density function.[31] Two kinds of basis sets were used. A smaller system (BS-I) was employed in geometry optimization. In the BS-I system, core electrons of platinum were replaced with effective core potentials (ECPs), where a (341/321/21) basis set were employed for valence electrons of platinum.[32] For P, S and acetylenic carbon atoms, usual 6-31G(d) basis sets were employed.[33] For other C and H, 6-31G basis sets were employed. The better basis set system (BS-II) was employed to evaluate the excited states and oscillator strengths by the TD-B3LYP method. In the BS-II system, core electrons of platinum were replaced with effective core potentials (ECPs), where a (541/5511/211) basis set was employed for valence electrons of platinum.[34] For other atoms, the basis sets were the same as for BS-I.

Acknowledgements

This work was supported by Grant-in-Aids for Scientific Research on Priority Areas "Synergy of Elements" and "Molecular Theory for Real Systems" from MEXT, Japan.

Notes and references

1 P. Le Floch, *Coord. Chem. Rev.*, 2006, **250**, 627; M. Yoshifuji, *Pure Appl. Chem.*, 2005, **77**, 2011; F. Mathey, *Angew. Chem., Int. Ed.*, 2003, **42**, 1578; L. Weber, *Angew. Chem., Int. Ed.*, 2002, **41**, 563; L. Weber, *Coord. Chem. Rev.*, 2005, **249**, 741; C. Müller and D. Vogt, *Dalton Trans.*, 2007, 5505.
2 F. Ozawa and M. Yoshifuji, *Dalton Trans.*, 2006, 4987; F. Ozawa and M. Yoshifuji, *C. R. Chimie*, 2004, **7**, 747.
3 T. Minami, H. Okamoto, S. Ikeda, R. Tanaka, F. Ozawa and M. Yoshifuji, *Angew. Chem., Int. Ed.*, 2001, **40**, 4501.
4 F. Ozawa, H. Okamoto, S. Kawagishi, S. Yamamoto, T. Minami and M. Yoshifuji, *J. Am. Chem. Soc.*, 2002, **124**, 10968; F. Ozawa, T. Ishiyama, S. Yamamoto, S. Kawagishi, H. Murakami and M. Yoshifuji, *Organometallics*, 2004, **23**, 1698; H. Murakami, T. Minami and F. Ozawa, *J. Org. Chem.*, 2004, **69**, 4482; H. Murakami, Y. Matsui, F. Ozawa and M. Yoshifuji, *J. Organomet. Chem.*, 2006, **691**, 3151.
5 R. S. Jensen, K. Umeda, M. Okazaki, F. Ozawa and M. Yoshifuji, *J. Organomet. Chem.*, 2007, **692**, 286.
6 H. Katayama, M. Nagao, T. Nishimura, Y. Matsui, K. Umeda, K. Akamatsu, T. Tsuruoka, H. Nawafune and F. Ozawa, *J. Am. Chem. Soc.*, 2005, **127**, 4350; M. Nagao, K. Asano, K. Umeda, H. Katayama and F. Ozawa, *J. Org. Chem.*, 2005, **70**, 10511; A. Hayashi, T. Yoshitomi, K. Umeda, M. Okazaki and F. Ozawa, *Organometallics*, 2008, **27**, 2321.
7 F. Ozawa, S. Kawagishi, T. Ishiyama and M. Yoshifuji, *Organometallics*, 2004, **23**, 1325.
8 K. Hayashi, M. Nakatani, A. Hayashi, M. Takano, M. Okazaki, K. Toyota, M. Yoshifuji and F. Ozawa, *Organometallics*, 2008, **27**, 1970.
9 G. Frenking and N. Fröhlich, *Chem. Rev.*, 2000, **100**, 717; C. Massera and G. Frenking, *Organometallics*, 2003, **22**, 2758; M. Piacenza, J. Rakow, I. Hyla-Kryspin and S. Grimme, *Eur. J. Inorg. Chem.*, 2006, 213, and references cited therein.
10 H. Meier, *Angew. Chem., Int. Ed.*, 2005, **44**, 2482; Y. Matano, K. Matsumoto, Y. Nakao, H. Uno, S. Sakaki and H. Imahori, *J. Am. Chem. Soc.*, 2008, **130**, 4588.
11 N. Robertson and L. Cronin, *Coord. Chem. Rev.*, 2002, **227**, 93; A. E. Pullen and R.-M. Olk, *Coord. Chem. Rev.*, 1999, **188**, 211.
12 The synthetic procedure followed the preparation of [Pt(alkyne)L_2] complexes (L = PMe_3, PEt_3 and PPh_3): N. M. Boag, M. Green, D. M. Grove, J. A. K. Howard, J. L. Spencer and F. G. A. Stone, *J. Chem. Soc.,Dalton Trans.*, 1980, 2170.
13 The X-ray structure of [Pt(tolan-H)(DPCB-H)] was determined in this study.

14 [Pt(tolan-H)(dppbz)]: H. Petzold, H. Görls and W. Weigand, *J. Organomet. Chem.*, 2007, **692**, 2736.
15 [Pt(tolan-H)(dppp)]: K. Zhang, J. Hu, K. C. Chan, K. Y. Wong and J. H. K. Yip, *Eur. J. Inorg. Chem.*, 2007, 384.
16 [Pt(tolan-H)(PPh_3)$_2$]: K. J. Harris, G. M. Bernard, C. McDonald, R. McDonald, M. J. Ferguson and R. E. Wasylishen, *Inorg. Chem.*, 2006, **45**, 2461.
17 B. W. Davies and N. C. Payne, *Inorg. Chem.*, 1974, **13**, 1848; J. F. Richardson and N. C. Payne, *Can. J. Chem.*, 1977, **55**, 3203.
18 N. Inamoto, *Hammett Rule*, Maruzen, Tokyo, 1983.
19 [$PtMe_2$(dppe)]: D. C. Smith, Jr., C. M. Haar, E. D. Stevens, S. P. Nolan, W. J. Marshall and K. G. Moloy, *Organometallics*, 2000, **19**, 1427; S. Jxietkamp, D. J. Stufkens and K. Vrieze, *J. Organomet. Chem.*, 1979, **169**, 107.
20 [Pt(bdt-NNtol)(dppe)]: M. Nihei, M. Kurihara, J. Mizutani and H. Nishihara, *Chem. Lett.*, 2001, 852.
21 [Pt(bdt)(dppf)]: L. L. Maisela, A. M. Crouch, J. Darkwa and I. A. Guzei, *Polyhedron*, 2001, **20**, 3189.
22 [Pt(bdt)(mesBIAN)]: C. J. Adams, N. Fey, M. Parfitt, S. J. A. Popeb and J. A. Weinstein, *Dalton Trans.*, 2007, 4446.
23 [Pt(bdt)(bipy)]: W. B. Connick and H. B. Gray, *J. Am. Chem. Soc.*, 1997, **119**, 11620.
24 [Pt(bdt-t-Bu_2)(phen-Ph_2)]: J. A. Weinstein, M. T. Tierney, E. S. Davies, K. Base, A. A. Robeiro and M. W. Grinstaff, *Inorg. Chem.*, 2006, **45**, 4544.
25 The X-ray structure of [$PtCl_2$(DPCB-H)] was determined in this study.
26 [$PtCl_2$(dppe)]: D. H. Farrar and G. Ferguson, *J. Crystallogr. Spectrosc. Res.*, 1982, **12**, 465; E. G. Hope, W. Levason and N. A. Powell, *Inorg. Chim. Acta*, 1986, **115**, 187.
27 A. Nakamura, S. Kawasaki, K. Toyota and M. Yoshifuji, *Chem. Lett.*, 2004, **33**, 1570.
28 J. L. Spencer, *Inorg. Synth.*, 1979, **19**, 213.
29 T. Hansen, J. Becher, T. Jørgensen, K. S. Varma, R. Khedekar and M. Cava, *Org. Synth.*, 1996, **73**, 270.
30 G. M. Sheldrick, *SHELX-97*, University of Göttingen, Germany, 1997.
31 M. J. Frisch, G. W. Trucks, H. B. Schlegel, G. E. Scuseria, M. A. Robb, J. R. Cheeseman, J. A. Montgomery, Jr., T. Vreven, K. N. Kudin, J. C. Burant, J. M. Millam, S. S. Iyengar, J. Tomasi, V. Barone, B. Mennucci, M. Cossi, G. Scalmani, N. Rega, G. A. Petersson, H. Nakatsuji, M. Hada, M. Ehara, K. Toyota, R. Fukuda, J. Hasegawa, M. Ishida, T. Nakajima, Y. Honda, O. Kitao, H. Nakai, M. Klene, X. Li, J. E. Knox, H. P. Hratchian, J. B. Cross, V. Bakken, C. Adamo, J. Jaramillo, R. Gomperts, R. E. Stratmann, O. Yazyev, A. J. Austin, R. Cammi, C. Pomelli, J. Ochterski, P. Y. Ayala, K. Morokuma, G. A. Voth, P. Salvador, J. J. Dannenberg, V. G. Zakrzewski, S. Dapprich, A. D. Daniels, M. C. Strain, O. Farkas, D. K. Malick, A. D. Rabuck, K. Raghavachari, J. B. Foresman, J. V. Ortiz, Q. Cui, A. G. Baboul, S. Clifford, J. Cioslowski, B. B. Stefanov, G. Liu, A. Liashenko, P. Piskorz, I. Komaromi, R. L. Martin, D. J. Fox, T. Keith, M. A. Al-Laham, C. Y. Peng, A. Nanayakkara, M. Challacombe, P. M. W. Gill, B. G. Johnson, W. Chen, M. W. Wong, C. Gonzalez and J. A. Pople, *GAUSSIAN 03 (Revision C.02)*, Gaussian, Inc., Wallingford, CT, 2004.
32 P. J. Hay and W. R. Wadt, *J. Chem. Phys.*, 1985, **82**, 299.
33 W. J. Hehre, R. Ditchfield and J. A. Pople, *J. Chem. Phys.*, 1972, **56**, 2257.
34 M. Couty and M. B. Hall, *J. Comput. Chem.*, 1996, **17**, 1359; R. B. Ross, J. M. Powers, T. Atashroo, W. C. Ermler, L. A. LaJohn and P. A. Christiansen, *J. Chem. Phys.*, 1990, **93**, 6654.

